nature chemical biology

ARTICLE

PUBLISHED ONLINE: 15 APRIL 2012 | DOI: 10.1038/NCHEMBIO.937

Trp-tRNA synthetase bridges DNA-PKcs to PARP-1 to link IFN-γ and p53 signaling

Mathew Sajish[1], Quansheng Zhou[1,4], Shuji Kishi[2], Delgado M Valdez Jr[2], Mili Kapoor[1,4], Min Guo[2], Sunhee Lee[1,3,4], Sunghoon Kim[3], Xiang-Lei Yang[1] & Paul Schimmel[1]*

Interferon-γ (IFN-γ) engenders strong antiproliferative responses, in part through activation of p53. However, the long-known IFN-γ–dependent upregulation of human Trp-tRNA synthetase (TrpRS), a cytoplasmic enzyme that activates tryptophan to form Trp-AMP in the first step of protein synthesis, is unexplained. Here we report a nuclear complex of TrpRS with the catalytic subunit of DNA-dependent protein kinase (DNA-PKcs) and with poly(ADP-ribose) polymerase 1 (PARP-1), the major PARP in human cells. The IFN-γ–dependent poly(ADP-ribosyl)ation of DNA-PKcs (which activates its kinase function) and concomitant activation of the tumor suppressor p53 were specifically prevented by Trp-SA, an analog of Trp-AMP that disrupted the TrpRS–DNA-PKcs–PARP-1 complex. The connection of TrpRS to p53 signaling *in vivo* was confirmed in a vertebrate system. These and further results suggest an unexpected evolutionary expansion of the protein synthesis apparatus to a nuclear role that links major signaling pathways.

Aminoacyl-tRNA synthetases are universal ancient proteins that establish the rules of the genetic code through specific aminoacylation of tRNAs, which constitutes the first step of translation[1]. The 20 enzymes (one for each amino acid) are divided into two classes (I and II) according to the architecture of the active site for synthesis of aminoacyl-AMP, which is transferred to the 3′ end of tRNA[2,3]. We were especially interested in the long-standing observation that the class I human TrpRS is highly induced by IFN-γ[4–6]. IFN-γ is associated with strong antiproliferative[7] and antiangiogenic effects[8] and the activation of p53 through phosphorylation of Ser15 (ref. 9). In addition to TrpRS, IFN-γ stimulates production of other angiostatic factors such as MIG[10] and IP10 (ref. 11). Though TrpRS is mainly located in the cytoplasm, under IFN-γ stimulation it is secreted, and its embedded antiangiogenic function is activated by removal of an appended N-terminal domain (by proteolytic processing or alternative splicing)[12,13]. The activated form of TrpRS binds vascular endothelial cadherin on the surface of endothelial cells and inhibits the formation of cadherin-mediated endothelial cell-cell junctions that are critical for vasculature development[14].

In addition to these considerations, the observation that eukaryotic tRNA synthetases have progressively (in evolution) added domains that are often not associated with their canonical aminoacylation function were of much interest to us[15]. The WHEP domain is a common appended helix-turn-helix motif found in a number of human tRNA synthetases including TrpRS, HisRS, the bifunctional Glu-ProRS, GlyRS and MetRS[15]. The three WHEP domains in Glu-ProRS were found to mediate protein-protein and protein-RNA interactions that regulate translation of genes associated with the inflammatory response[16]. Separately, recent work showed that human LysRS is phosphorylated in stimulated mast cells[17]. Phosphorylation releases LysRS from the multi–tRNA synthetase complex in the cytoplasm and redirects the protein to the nucleus, where it interacts with the microphthalmia-associated transcription factor to activate transcription of genes that control the immune response. These observations show that at least some tRNA synthetases, long thought to have a role only in translation in the cytoplasm, have distinct ex-translational nuclear functions. Hence, it remained a subject of investigations to determine whether these functions originated from the need to coordinate these nuclear signaling pathways with translation in the cytoplasm. In this aspect, we were interested in the previously reported nuclear presence of TrpRS[18,19], which was suggestive of a possible new nuclear function for TrpRS.

Here we find that, upon IFN-γ stimulation, nuclear TrpRS increases in concentration and appears in a complex in which it serves as a bridge between the catalytic subunit of DNA-PKcs and PARP-1. The subsequent cascade of biochemical events that results from this ternary complex leads to activation of p53. Notably, a previously uncharacterized domain, which is dispensable for aminoacylation, was added to the N terminus of TrpRS at the time of vertebrate evolution and seems to be essential for enabling TrpRS to link IFN-γ and p53 signaling.

RESULTS

Nuclear partners of TrpRS

As IFN-γ is known to upregulate TrpRS expression[4–6], we started our investigation by analyzing the effect of IFN-γ stimulation on TrpRS nuclear localization. Under normal conditions, little TrpRS could be detected in the nuclear fraction of 3B11 cells (an immortal B-cell line) (**Supplementary Results**, **Supplementary Fig. 1a**). However, upon IFN-γ treatment, the presence of TrpRS in the nucleus, along with its overexpression in the cytoplasm, was easily detected in a variety of cell lines (**Supplementary Fig. 1b**). This observation demonstrated that IFN-γ–mediated upregulation and translocation of TrpRS into the nucleus was not specific to a particular cell line. Notably, plasmid-based transient overexpression of TrpRS alone also led to its nuclear localization (**Supplementary Fig. 1c**). Confocal

[1]The Skaggs Institute for Chemical Biology, Department of Molecular Biology, The Scripps Research Institute, La Jolla, California, USA. [2]The Scripps Research Institute, Jupiter, Florida, USA. [3]Department of Molecular Medicine and Biopharmaceutical Sciences, Medicinal Bioconvergence Research Center, World Class University, Seoul National University, Seoul, Korea. [4]Present addresses: Cyrus Tang Hematology Center, Jiangsu Institute of Hematology, The First Affiliated Hospital of Soochow University, Soochow University, Suzhou, Jiangsu, China (Q.Z.); Anaphore, Inc., La Jolla, California, USA (M.K.); Department of Molecular Cell and Developmental Biology, Institute for Cellular and Molecular Biology, University of Texas, Austin, Texas, USA (S.L.). *e-mail: schimmel@scripps.edu

microscopy also demonstrated the nuclear localization of TrpRS during IFN-γ stimulation (**Supplementary Fig. 1d**) or upon ectopic overexpression (**Supplementary Fig. 1e**). In addition to other possible effects from IFN-γ stimulation, this observation suggested that nuclear localization was detected because of increased expression of TrpRS and the possibility of a nuclear localization signal (NLS) in the primary sequence. A multiple-sequence alignment revealed four potential bipartite NLS elements near the C terminus, sequentially designated as M1, M2, M3 and M4 (**Supplementary Fig. 1f**). Subsequent mutational analysis confirmed that human TrpRS contains a bipartite NLS, ^{448}RRKEVTDEIVKEFMTPRK^{465} (M3 and M4 are underlined), that is responsible for its nuclear import (**Supplementary Fig. 1g**).

Having identified the NLS of TrpRS, we attempted to identify potential nuclear partners for TrpRS. The nuclear fraction from HeLa cells that were treated with IFN-γ was isolated, and a coimmunoprecipitation was performed using polyclonal antibodies specific for TrpRS (anti-TrpRS). An MS identification of the immunoprecipitated proteins yielded DNA-PKcs (465 kDa) and PARP-1 (110 kDa) as major potential interacting partners (**Fig. 1a**). The identities of DNA-PKcs and PARP-1 and their interaction with TrpRS were also confirmed by reverse coimmunoprecipitation with antibodies specific for DNA-PKcs (anti-DNA-PKcs) and PARP-1 (anti-PARP1) (**Supplementary Fig. 2b**).

WHEP domain needed for TrpRS–DNA-PK–PARP-1 interaction

As a class I tRNA synthetase, TrpRS from any organism contains the conserved Rossmann-fold catalytic and anticodon-binding domains[20,21]. In addition, human TrpRS has a vertebrate-specific helix-turn-helix WHEP domain (~60 amino acids) appended at the N terminus[15]. The WHEP domain is completely disordered in the cocrystal structure of the human TrpRS–tRNA complex[21], consistent with its dispensability in aminoacylation[20]. The flexible conformation of the WHEP domain suggested that it may be important for interactions with other partners. To test whether the WHEP domain is involved with the interaction with PARP-1 and DNA-PKcs, we used two natural variants lacking the WHEP domain. One was mini-TrpRS (residues 48–471), and the other was T2-TrpRS (residues 94–471). The former is produced by alternative splicing[22] and the latter by natural proteolysis[12]. Two additional constructs were the N-terminal fragment NT-TrpRS (residues 1–186), which covers the entire eukaryote-specific region of TrpRS[20,21], and the WHEP domain by itself (residues 1–60). Nickel-nitrilotriacetic acid (Ni-NTA) pull-down experiments with these histidine-tagged proteins showed that neither mini- nor T2-TrpRS interacted with PARP-1 or DNA-PKcs. In contrast, both NT-TrpRS and the WHEP domain interacted with PARP-1 and DNA-PKcs (**Fig. 1b**). Thus, the WHEP domain of TrpRS is responsible and sufficient for mediating the interaction with DNA-PKcs and PARP-1.

To understand the determinants on DNA-PKcs that interact with TrpRS, three different constructs of the 4,128-amino-acid DNA-PKcs were also created. These constructs were based largely on predicted domain boundaries in the sequence[23]. Only the fragment containing the V5-tagged C-terminal kinase domain of DNA-PKcs (V5-KD-DNA-PKcs) interacted with TrpRS (**Fig. 1c**). Neither the N-terminal (residues 1–1025; NT-DNA-PKcs) nor the middle (residues 1000–2184; MD-DNA-PKcs) portions of DNA-PKcs interacted with TrpRS (**Fig. 1c**), thus suggesting that the C-terminal kinase region of DNA-PKcs is responsible for the interaction.

Although DNA-PKcs and PARP-1 are substrates for each other[24], it is remarkable that purified DNA-PKcs and PARP-1 do not interact *in vitro*[25]. Hence, their interaction is believed to be mediated through the heterodimer formed by Ku70 and Ku80 (Ku70/80), the cofactor of DNA-PKcs in DNA repair that specifically binds damaged DNA[26]. However Ku70/80 was not seen in our MS analysis. These observations led us to consider TrpRS as an alternative functional bridge

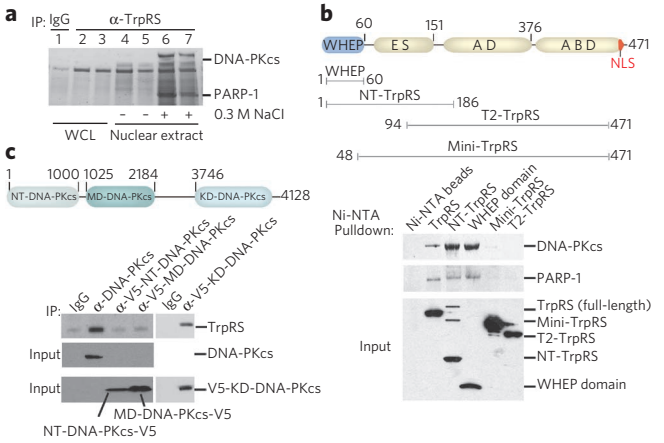

Figure 1 | Identification of DNA-PKcs and PARP-1 as nuclear interacting partners of TrpRS. (**a**) SDS-PAGE gel showing protein bands that were coimmunoprecipitated with anti-TrpRS from HeLa cells treated with IFN-γ (lysates (WCL) or nuclear extracts (duplicate lanes: 2 and 3, cytoplasmic fraction; 4 and 5, nuclear fraction without NaCl; 6 and 7, nuclear fraction with NaCl) or with IgG control (lane 1). Full-length gels are presented in **Supplementary Figure 2a**. IP, immunoprecipitation. (**b**) Mapping of the interaction domain on TrpRS. Schematic representation of human TrpRS domain constructs is depicted at the top. At the bottom is a Ni-NTA pull-down experiment showing that the WHEP domain of TrpRS was responsible for the interaction with DNA-PKcs and PARP-1. DNA-PKcs (and PARP-1) was found to interact with full-length and NT-TrpRS and with the WHEP domain alone, but not with mini- and T2-TrpRS. ES, eukaryote specific; AD, aminoacylation domain; ABD, anticodon-binding domain. (**c**) Mapping of the interaction domain on DNA-PK. A schematic representation of DNA-PKcs domain constructs is depicted at the top. Immunoprecipitation experiment showing the interaction of the kinase domain of DNA-PKcs (KD-DNA-PKcs) with TrpRS. N-terminal (NT-DNA-PKcs) and middle-domain (MD-DNA-PKcs) regions of DNA-PKcs do not interact with TrpRS.

such that a DNA-PKcs–TrpRS–PARP-1 ternary complex may form independently of DNA damage. (In experiments described later, we established that DNA-PKcs and PARP-1 formed a ternary complex, and not just separate binary complexes, with TrpRS.) To explore this idea, we prepared HeLa cell lysates and first confirmed that endogenous DNA-PKcs, PARP-1 and Ku70/80 could be coimmunoprecipitated with antibodies directed against Ku70 (anti-Ku70) (**Fig. 2a**). Although the DNA-PKcs–Ku70/80–PARP-1 complex was readily detected, it contained no endogenous TrpRS. Conversely, immunoprecipitation with anti-TrpRS pulled down DNA-PKcs and PARP-1, as expected, but revealed no detectable Ku70/80 (**Fig. 2a**). These experiments confirmed our MS analysis showing the absence of Ku70 and Ku80 from the TrpRS–DNA-PKcs–PARP-1 complex and suggested that the binding of TrpRS and Ku70/80 to DNA-PKcs and PARP-1 is mutually exclusive.

Distinct PARP-1 domains interact with TrpRS and Ku70/80

The mutually exclusive nature of the two complexes, along with the observation that both TrpRS (**Fig. 1c**) and Ku70/80 (ref. 27) interact with the C-terminal region harboring the kinase domain of DNA-PKcs, prompted us to further characterize the domain-specific interactions of PARP-1 with TrpRS and Ku70/80. N-terminal (residues 1–372; NTD-PARP-1) and C-terminal (catalytic; residues 661–1014; CTD-PARP-1) domains of PARP-1 were each cloned with a histidine tag and expressed in *Escherichia coli*. Ni-NTA pull-down experiments showed distinct interactions of Ku70/80 and TrpRS with PARP-1 in mixtures of bacterial extracts with HeLa cell

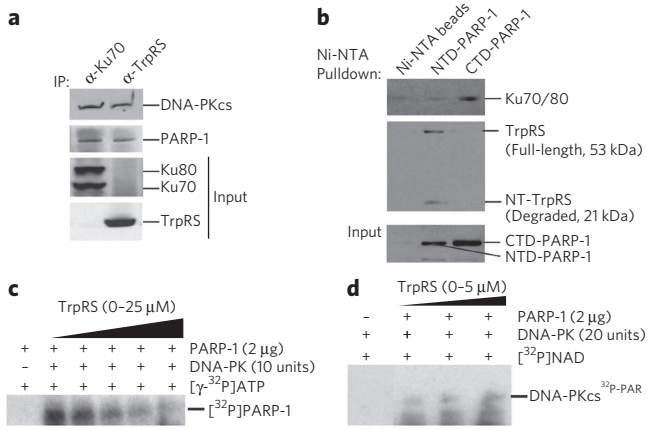

Figure 2 | TrpRS facilitates the poly(ADP-ribosy)lation of DNA-PKcs. (**a**) Mutually exclusive binding of TrpRS, and Ku70/80 to DNA-PKcs and PARP-1. Coimmunoprecipitation experiments were performed with anti-TrpRS or anti-Ku70 incubated with HeLa cell lysates. The proteins that were bound with the antibodies were separated by SDS-PAGE and immunoblotted with anti-DNA-PKcs, anti-PARP-1, anti-Ku70/80 and anti-TrpRS. TrpRS did not coimmunoprecipitate with Ku70/80 and vice versa. (**b**) Ni-NTA pull-down experiment showing domain-specific interaction of PARP-1 with TrpRS and with Ku80. TrpRS interacted with the N-terminal domain (NTD-PARP-1), and Ku70/80 interacted with the C-terminal domain (CTD-PARP-1). (**c**) TrpRS downregulated DNA-PK–dependent phosphorylation of PARP-1 *in vitro* in a concentration-dependent manner. DNA-PK (10 units) was incubated with a series of TrpRS concentrations for 30 min in a protein kinase assay. The phosphorylated [^{32}P]PARP-1 was separated from free [γ-^{32}P]ATP by SDS-PAGE and visualized by exposure to X-ray film. Full-length blots are presented in **Supplementary Figure 2d**. (**d**) *In vitro* demonstration of the ability of TrpRS to facilitate the PARylation of DNA-PKcs. Purified DNA-PK and purified recombinant PARP-1 were mixed with [^{32}P]NAD and incubated with an increasing concentration of TrpRS (up to 5 μM) in the reaction mixture. [^{32}P]PARylated DNA-PKcs was detected after running an SDS-PAGE and using X-ray film (full-length blots are presented in **Supplementary Fig. 2e**).

lysates; Ku70/80 interacted with the catalytic domain of PARP-1 (CTD-PARP-1), and TrpRS interacted with the N-terminal region (NTD-PARP-1) (**Fig. 2b**). Notably, an N-terminal WHEP domain–containing degradation fragment of TrpRS was also found to be eluted together with NTD-PARP-1 (**Fig. 2b**). This observation is consistent with the conclusion that the N-terminal WHEP domain is responsible for mediating the interaction with DNA-PKcs and PARP-1. Therefore, the potential ternary complex of DNA-PKcs–TrpRS–PARP-1 seems to be formed through the WHEP domain of TrpRS bridging the kinase domain of DNA-PKcs to the N-terminal domain of PARP-1.

Although purified DNA-PKcs and PARP-1 do not interact *in vitro*[25], DNA-PK is known to phosphorylate PARP-1 (ref. 24) in a reaction possibly facilitated by Ku70/80 bridging PARP-1 to the kinase domain of DNA-PKcs[27]. Because we found that Ku70/80 interacts with the C-terminal catalytic domain of PARP-1, we wondered whether CTD-PARP-1 contained the phosphorylation site for DNA-PK. To test this idea, we carried out an *in vitro* DNA-PK (containing Ku70/80 and double-stranded DNA) kinase assay using the different domains of PARP-1. As expected, only CTD-PARP-1 (and not NTD-PARP-1) was phosphorylated (**Supplementary Fig. 2c**). Therefore, through its interaction with Ku70/80 in the presence of dsDNA, DNA-PK phosphorylated PARP-1 at its catalytic CTD. This result is consistent with an earlier report that the major phosphorylation sites for DNA-PK are at the C-terminal domain of PARP-1 (ref. 24). In contrast, TrpRS seemed to bridge the N-terminal region of PARP-1 to the kinase domain of DNA-PKcs. Thus, Ku70/80 and TrpRS differ in the way they orient PARP-1 with respect to DNA-PKcs.

Effect of TrpRS on modifications of PARP-1 and DNA-PKcs

Once phosphorylated by DNA-PKcs, PARP-1 cannot poly(ADP-ribosyl)ate (PARylate) DNA-PKcs[24]. Because of the inverse relationship between the phosphorylation status of PARP-1 and its ability to PARylate DNA-PKcs, we were interested to see whether TrpRS can influence the DNA-PKcs–dependent phosphorylation of PARP-1 and, conversely, the PARP-1–dependent PARylation of DNA-PKcs. For this purpose, we performed *in vitro* kinase and PARylation assays. In the kinase assay PARP-1 was the substrate for DNA-PKcs, and in the PARylation assay DNA-PKcs was the substrate for PARP-1. As expected, TrpRS inhibited the DNA-PKcs–mediated phosphorylation of PARP-1 (**Fig. 2c**) and facilitated the PARylation of DNA-PKcs (**Fig. 2d**).

Having demonstrated *in vitro* that TrpRS facilitates the PARylation of DNA-PKcs (DNA-PKcs^{PAR}) and inhibits the phosphorylation of PARP-1, we wanted to see whether similar effects occurred *in vivo* when TrpRS was overexpressed in the absence of IFN-γ stimulation. For this purpose, V5-tagged TrpRS (TrpRS-V5) was ectopically overexpressed in HeLa cells, and this overexpression resulted in substantial PARylation of DNA-PKcs (**Fig. 3a**, left). Consistently with transient overexpression of TrpRS alone, IFN-γ stimulation to upregulate endogenous TrpRS also resulted in strong PARylation of DNA-PKcs (**Fig. 3a**, right). Furthermore, in an IgG pull-down experiment using ZZ-PARP-1 (a fusion protein of PARP-1 with an IgG-binding domain of protein A (ZZ) at the N terminus) with ectopically expressed TrpRS-V5, PARP-1–associated DNA-PKcs was also PARylated. In contrast, without overexpression of TrpRS-V5, PARP-1–associated DNA-PKcs (through Ku70/80) was mostly unmodified (**Fig. 3b**).

Similarly, to demonstrate the influence of TrpRS overexpression on the *in vivo* phosphorylation of PARP-1, we transfected ZZ-PARP-1 into HeLa cells together with genes encoding either TrpRS-V5 or V5-tagged TrpRS with an additional NLS (KKKRKV) appended to the C terminus (TrpRS^{NLS}-V5). The rationale for using TrpRS^{NLS}-V5 was that the enhanced nuclear localization of TrpRS, in the absence of IFN-γ stimulation, should result in a greater response than that achieved with wild-type TrpRS alone. ZZ-PARP-1 from all three samples was pulled down using IgG and was blotted with antibodies to phosphorylated serine (DNA-PKcs is a serine/threonine protein kinase). Diminished phosphorylation of ZZ-PARP-1 was observed when V5-TrpRS was coexpressed, and this diminution was even greater with TrpRS^{NLS}-V5 (**Fig. 3c**). Concomitantly, coexpression of TrpRS-V5 also diminished the binding of Ku70/80 to ZZ-PARP-1. This diminution was even more pronounced with TrpRS^{NLS}-V5 (**Fig. 3c**). These data support the idea that, when TrpRS displaces Ku70/80 and functionally bridges PARP-1 to DNA-PKcs, it facilitates PARylation of DNA-PKcs and downregulates the phosphorylation of PARP-1.

TrpRS facilitates phosphorylation of p53

As PARylation of DNA-PKcs (DNA-PKcs^{PAR}) is known to stimulate its kinase activity on p53 (ref. 25), we tested for p53 phosphorylation (at Ser15) *in vivo* under conditions in which TrpRS was overexpressed. p53 is a well-known substrate for DNA-PK both *in vitro*[28] and *in vivo*[29], and phosphorylation of p53 at Ser15 (pSer15) by DNA-PK (or other kinases with similar specificity; for example, ataxia telangiectasia mutated (ATM)) is required for its stabilization and activation[30]. As expected, IFN-γ stimulation to upregulate endogenous TrpRS resulted in strong PARylation of DNA-PKcs with concomitant phosphorylation (at Ser15) of p53 (**Fig. 3d**). Similarly, we found that ectopic overexpression of TrpRS, in the absence of IFN-γ stimulation, also resulted in activation of DNA-PKcs

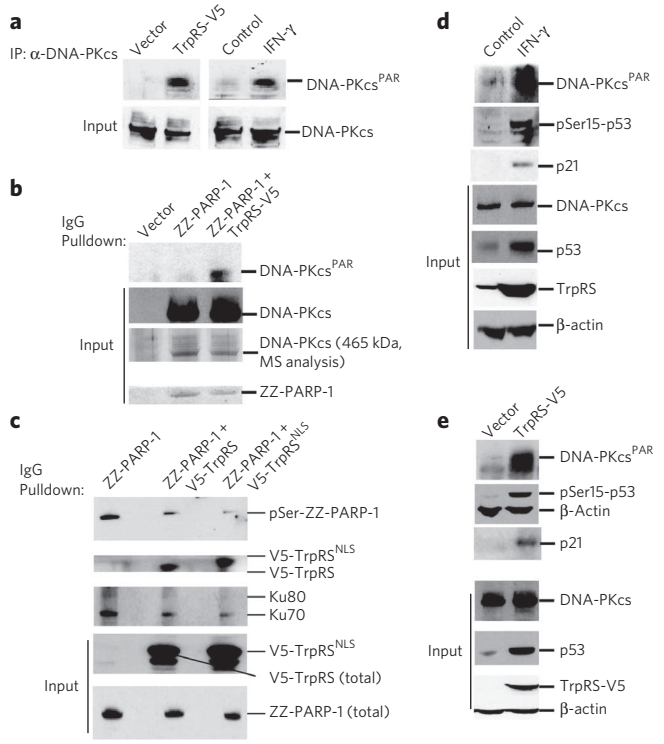

Figure 3 | TrpRS overexpression via transfection or IFN-γ stimulation activate DNA-PKcs and p53 by promoting DNA-PKcs PARylation. (**a**) Overexpression of TrpRS by transient transfection (left-most lane) or IFN-γ stimulation (right-most lane) led to the PARylation of DNA-PKcs, as shown by immunoblotting. (**b**) Bridging of DNA-PKcs with PARP-1 by TrpRS led to the PARylation of DNA-PKcs. Only the ZZ-PARP-1 pulled down from samples cotransfected with TrpRS-V5 contained the PARylated DNA-PKcs (upper two rows). The identity of the specific band as DNA-PKcs was confirmed by MS. Full-length blots and gels are presented in **Supplementary Figure 3**. (**c**) TrpRS downregulated the autophosphorylation of PARP-1. Top row shows the phosphorylation status (pSer) of the immunoprecipitated ZZ-PARP-1 from HeLa cells transfected with plasmids encoding either ZZ-PARP-1 alone or cotransfected with V5-TrpRS or V5-TrpRS^{NLS}). Displacement of Ku70/80 (third row) by overexpressed V5-TrpRS was demonstrated by the increased association of V5-TrpRS^{NLS} with the immunoprecipitated ZZ-PARP-1 (second row). (**d**) IFN-γ–stimulated overproduction of TrpRS also led to the activation of p53 and production of the downstream marker p21. The amount of total and poly(ADP)ribosylated DNA-PKcs (DNA-PKcs^{PAR}), phosphorylated p53 and p21 were probed by immunoblotting with specific antibodies. (**e**) *In vivo* overexpression of TrpRS in HeLa cells led to the activation of p53. The amount of total and poly(ADP)ribosylated DNA-PKcs (DNA-PKcs^{PAR}), total and phosphorylated p53 and p21 were probed by immunoblotting.

by PARP-1–mediated PARylation and the concomitant phosphorylation of p53 at Ser15 (**Fig. 3e**). In both instances (**Fig. 3d,e**), the upregulation of expression of p21 from a downstream target gene of pSer15-p53 was also observed. These results are consistent with previous work[25] in which PARylation of DNA-PKcs stimulated its kinase activity on p53 *in vitro*. As the phosphorylated form of PARP-1 is known to be proangiogenic[31] and activated p53 is known to be antiangiogenic[32], these results are also consistent with the anti-angiogenic role of secreted TrpRS.

Notably, although the WHEP domain was sufficient and necessary for the bridging of homodimeric TrpRS to PARP-1 and DNA-PKcs (**Fig. 1b**), overexpression of the WHEP domain alone did not result in PARylation of DNA-PKcs, even though a complex formed between the WHEP domain and DNA-PKcs (**Supplementary Fig. 4a**) and some of the WHEP domain could enter the nucleus (presumably owing to its small size; **Supplementary Fig. 4b**). These results suggested that the rest of TrpRS (which contains the active site for Trp-AMP synthesis and harbors the NLS) has a role in making a functional complex. Remarkably, a 'pulldown' of KD-DNA-PKcs simultaneously captures NTD-PARP-1 and dimeric TrpRS, and, conversely, a pulldown of NTD-PARP-1 simultaneously captures KD-DNA-PKcs and dimeric TrpRS (**Supplementary Fig. 4c**). This experiment clearly establishes that DNA-PKcs and PARP-1 form a ternary complex with TrpRS (as opposed to separate binary complexes). In contrast, we could not detect a ternary complex with the WHEP domain or with a rationally designed TrpRS monomer (**Supplementary Fig. 4d**). These results are consistent with a model in which DNA-PKcs binds to one and PARP-1 to the other WHEP domain of dimeric TrpRS.

To understand better the role of the WHEP domain in conjunction with the active site, we reexamined our previously obtained crystal structure of human TrpRS[20]. The structure captured the homodimeric TrpRS in a state of half-site reactivity in which the reaction intermediate Trp-AMP occupied one active site while the other active site was empty. Remarkably, when the active site was bound with Trp-AMP, the WHEP domain (**Fig. 4a**) was resolved in the crystal structure and folded back toward the active site as a cap, while, at the same time, the WHEP domain of the other subunit, which lacks bound Trp-AMP, was disordered along with the other residues with which it interacts. As the disposition of the WHEP domain may affect its availability for protein-protein interactions and is determined by the occupancy of the active site, we hypothesized that a bound ligand such as Trp-AMP could negatively affect the interaction of TrpRS with DNA-PKcs and PARP-1.

To test this idea, we used a nonhydrolyzable analog of Trp-AMP, 5′-*O*-[*N*-(L-tryptophanyl)sulfamoyl] adenosine (Trp-SA), and investigated its effect on DNA-PK and p53 activation. We added various amounts of Trp-SA into medium containing cultured cells that overexpressed either endogenous TrpRS (by IFN-γ stimulation) (**Fig. 4b**) or exogenous TrpRS-V5 (**Fig. 4c**). Notably, Trp-SA suppressed the PARylation of DNA-PKcs and the activation of p53 in a dose-dependent manner (**Fig. 4b,c**). The treatment with Trp-SA (for 2 h) did not affect expression of TrpRS, DNA-PKcs or β-actin (**Fig. 4b,c**) or the nuclear localization of TrpRS. Thus, although the active site of TrpRS is essential for protein synthesis, the partial inhibition of TrpRS activity by Trp-SA was not sufficient to reduce overall protein synthesis within a short period of time. This result is consistent with other work showing that cell and even animal survival can be supported by reduced tRNA synthetase activity[33]. Nevertheless, to rule out the possibility that the effects of Trp-SA on DNA-PK PARylation and p53 were caused by inhibition of protein synthesis, we used a nonhydrolyzable adenylate analog of glycyl-AMP (Gly-SA) as a control. Gly-SA (25 μM) did not suppress DNA-PK PARylation and did not diminish p53 phosphorylation, thus suggesting that the effect of Trp-SA was specific to TrpRS and independent of any general effect on protein synthesis (**Fig. 4d**). To further confirm this result, we used puromycin at a concentration (25 μM) known to inhibit protein synthesis in HeLa cells[34]. Puromycin, like Gly-SA, did not diminish the phosphorylation of p53, which occurred upon overexpression of TrpRS (**Supplementary Fig. 5c**). Addition of Trp-SA to whole cells, followed by preparation of lysates and immunoprecipitations, showed that Trp-SA acted by disrupting the interaction of TrpRS with DNA-PKcs and PARP-1 (**Fig. 4e**).

In further experiments, and in an attempt to link the production of pSer15-p53 to an activity dependent on DNA-PKcs, we used the DNA-PKcs–specific inhibitor KU57788, which is reported to have a >1,000-fold specificity for DNA-PKcs over other kinases, including ATM[35]. Overexpression of TrpRS in the presence of KU57788 sharply suppressed the phosphorylation of p53 (**Supplementary Fig. 5c**). Though we cannot exclude the possibility that KU57788

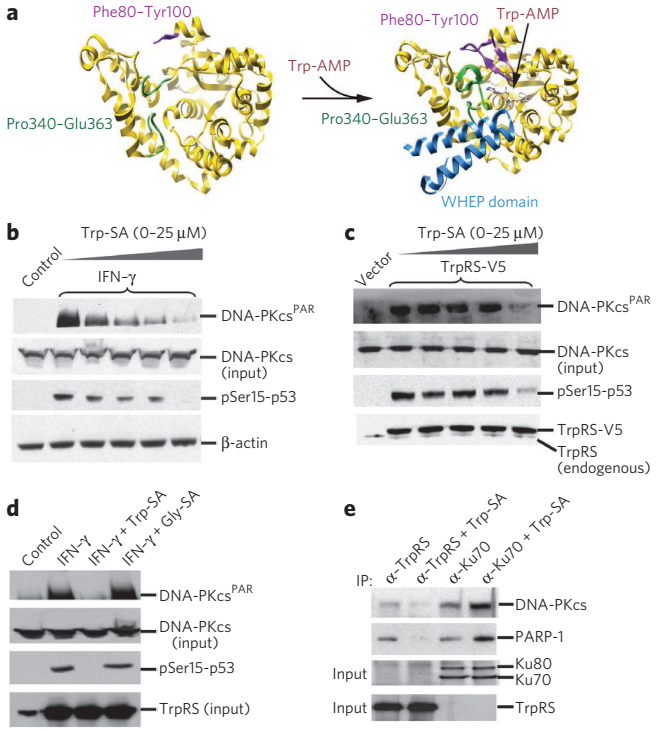

Figure 4 | Occupancy of TrpRS active site determines the WHEP domain conformation and dictates the DNA-PK–TrpRS–PARP-1 complex formation and associated activities. (**a**) Open (left) and closed (right) conformations of human TrpRS controlled by the binding of Trp-AMP. The human TrpRS structure was solved as a homodimer in the asymmetric unit (PDB code: 1R6T). One subunit in the asymmetric unit has a bound Trp-AMP in the active site (closed conformation), whereas the active site of the other subunit is empty (open conformation). The WHEP domain (blue), which is part of the eukaryote-specific patch (purple, Tyr83–Tyr100), and the loop harboring the KMSAS motif (green) are resolved only when Trp-AMP is bound. (**b**,**c**) Dose-dependent inhibition of Trp-SA on PARylation of DNA-PKcs and phosphorylation of p53 induced by TrpRS overexpression by IFN-γ stimulation (**b**) or by transient transfection (**c**). (**d**) Specificity of Trp-SA in inhibiting PARylation of DNA-PKcs and phosphorylation of p53 under IFN-γ stimulation. Full-length blots are presented in **Supplementary Figure 5a**,**b**. (**e**) Effect of Trp-SA on the interaction of TrpRS with DNA-PKcs and PARP-1. Coimmunoprecipitation experiments with anti-TrpRS and anti-Ku70, in the presence and absence of Trp-SA (50 μM), revealed that Trp-SA abolished the interaction of TrpRS with DNA-PKcs and PARP-1 and promoted association of DNA-PKcs and PARP-1 with Ku70/80. The observation is consistent with the idea that binding of Ku70/80 and TrpRS are mutually exclusive.

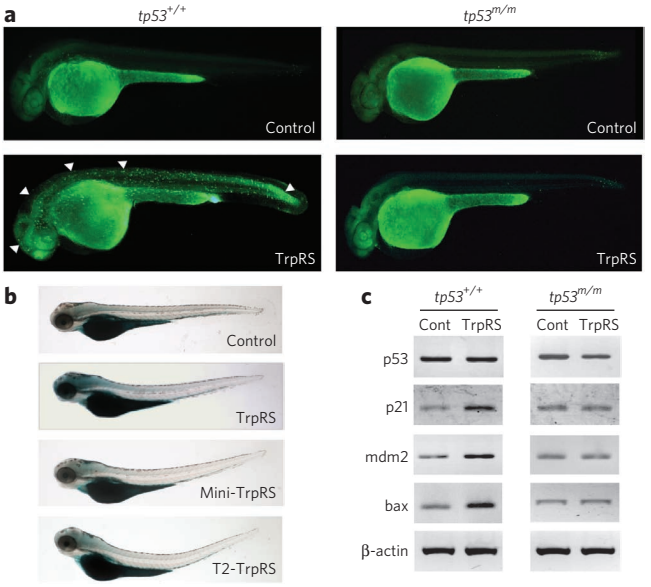

Figure 5 | TrpRS-mediated activation of p53 in zebrafish. (**a**) Acridine orange (AO) staining of live zebrafish embryos at 30 h.p.f. AO-positive fluorescent staining was observed in the brain, spinal cord, trunk and tail of *tp53*$^{+/+}$ embryos injected with TrpRS-encoding mRNA but was not observed in mutant p53 (*tp53*$^{m/m}$) embryos. Representative regions of AO-positive cells are indicated by white arrowheads. (**b**) SA-β-gal staining of embryos 3.5 d post fertilization. Embryos injected with TrpRS-encoding mRNA showed noticeable SA-β-gal induction in the brain and throughout the head, whereas mini-TrpRS and T2-TrpRS mRNAs as well as the control did not show any detectable changes. (**c**) Genes involved in the p53 downstream signaling pathway were analyzed semiquantitatively using reverse-transcription PCR in control embryos and in embryos injected with TrpRS-encoding mRNA.

inhibits an undefined kinase in addition to DNA-PKcs, the most straightforward interpretation is that DNA-PKcs has a role in the production of pSer15-p53 when TrpRS is overexpressed.

Moreover, the rise in total p53 that accompanies overexpression of TrpRS was associated with a similar rise in pSer15-p53. Because the rise in total p53 can be blocked by inhibitors directed toward TrpRS or DNA-PKcs, which in turn block production of pSer15-p53 (**Supplementary Fig. 5c**), we suggest that stabilization of p53 by phosphorylation at least partially explains the rise in total p53 that occurs upon overexpression of TrpRS. Finally, we compared the time course of PARylation of DNA-PKcs and that of the appearance of pSer15-p53 upon overexpression of recombinant (no IFN-γ treatment) or endogenous TrpRS (using IFN-γ induction) (**Supplementary Fig. 6**). These data showed that, whether by overexpression of exogenous (**Supplementary Fig. 6a**) or of endogenous (IFN-γ stimulation; **Supplementary Fig. 6b**) TrpRS, the amount of DNA-PKcs^{PAR} rises in a systematic way for the duration of the time course (28 h) in a way that follows the increase of TrpRS. The rises of total p53 and pSer15-p53 were more or less systematic and correlated to the amounts of TrpRS for the first 20 h.

Effect of TrpRS on p53 signaling *in vivo* in a vertebrate

The *in vitro* biochemical analysis and the cell-based assays showed the essential role of the WHEP domain for TrpRS-dependent p53 signaling. The WHEP domain was added to TrpRS in vertebrates at the time fish evolved[15]. The appearance of the new domains in tRNA synthetases correlates with their involvement in ex-translational biology in higher eukaryotes[15]. To assess the importance of this unique pathway at the animal level, we established an *in vivo* system in developing zebrafish (which are known to have IFN signaling pathways[36,37]). In these experiments, we replaced IFN-γ upregulation of TrpRS by directly injecting synthetic mRNAs encoding TrpRS, mini-TrpRS, T2-TrpRS and TrpRS^{NLS} into wild-type and p53 mutant (*tp53*$^{M214K/M214K}$, designated as *tp53*$^{m/m}$) zebrafish embryos[38]. We used these four constructs to test the effects of TrpRS and, if any, their dependence on the presence of the WHEP domain, which is lacking in mini-TrpRS and T2-TrpRS (**Fig. 5** and **Supplementary Fig. 7**). The phenotypic consequences and specific expressions of p53-dependent downstream genes (to monitor p53 activation) were then observed, within a few days, in the context of the whole organism.

Synthetic mRNA encoding green fluorescent protein (GFP) was introduced as an injection control in addition to uninjected control embryos. Embryos injected with TrpRS-encoding mRNA showed cell death in the developing brain and neural tube at 30 h post fertilization (h.p.f.) (**Fig. 5a**). Out of 30 embryos injected with

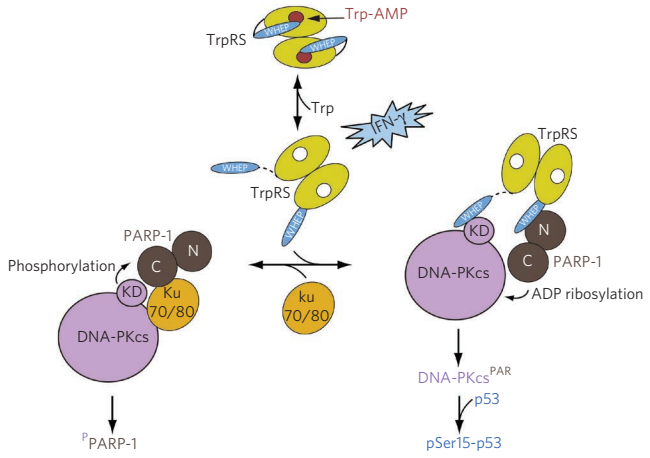

Figure 6 | Illustration of the nuclear function of TrpRS. In the absence of nuclear TrpRS, Ku70/80 bridges between DNA-PK and PARP-1 and orients the C-terminal domain (C) of PARP-1 for phosphorylation by DNA-PKcs. In the presence of nuclear TrpRS, Ku70/80 is displaced through the WHEP domain that bridges the C-terminal kinase domain (KD) of DNA-PKcs to the N-terminal domain (N) of PARP-1. Consequently, nuclear TrpRS stimulates PARsylation of DNA-PKcs and, in turn, the DNA-PKcs kinase activity that leads to p53 phosphorylation and activation. Because TrpRS excludes Ku70/80 from binding DNA-PKcs and PARP-1, it also inhibits Ku70/80–mediated PARP-1 phosphorylation by DNA-PKcs. The ability of TrpRS to bind DNA-PKcs and PARP-1 is controlled by the occupancy of the active site. Only when the active site is not occupied can the WHEP domain be opened and available for interaction with DNA-PKcs and PARP-1. ^{P}PARP-1, phosphorylated PARP-1.

TrpRS-encoding mRNA, 26 gave positive results; that is, ~80% of the total embryos responded positively to the injection. Some of the fish embryos had severely abnormal phenotypes, which were not counted as positive. In contrast, no abnormalities were observed in embryos injected with GFP-encoding mRNA. In addition, injection of mRNA encoding either mini- or T2-TrpRS did not induce detectable cell death. Notably, TrpRS-induced cell death was suppressed by the p53 mutant (*tp53*$^{m/m}$) background (**Fig. 5a**) as well as by co-injection of a p53-directed morpholino. These results in the vertebrate model supported the cell-based observations that WHEP domain–containing TrpRS regulates p53-mediated cell death signaling.

To further study the activation of p53, we stained zebrafish embryos for senescence-associated β-galactosidase (SA-β-gal), a marker that is upregulated by p53-induced cellular senescence *in vivo*[39,40]. As shown in **Figure 5b**, the staining was especially prominent in the head region of the developing embryos that were injected with TrpRS mRNA. In contrast, the intensity was greatly reduced in control embryos and in those injected with mini- or T2-TrpRS mRNA. These effects of injection of TrpRS RNA were greatly reduced in *tp53*$^{m/m}$ zebrafish (**Supplementary Fig. 7a**).

We then determined the expression of zebrafish p53, p21$^{WAF1/CIP1}$, mdm2 and bax relative to β-actin as a control. Semiquantitative reverse-transcription PCR was performed on RNA extracted from individual mRNA-injected embryos. When comparing wild-type and control-injected embryos, we were unable to detect any obvious change of p53 mRNA levels in embryos injected with TrpRS-encoding RNA (**Fig. 5c**). However, consistently with p53 activation, downstream targets of the p53 pathway such as mdm2, p21$^{WAF1/CIP1}$ and bax were correspondingly upregulated in wild-type (normal) p53 embryos injected with TrpRS-encoding mRNA (**Fig. 5c**, left). More importantly, the upregulation of mdm2, p21$^{WAF1/CIP}$ and bax was counteracted in p53 mutant fish embryos (**Fig. 5c**, right). In further support of the role of TrpRS as a component of p53 signaling, TrpRS^{NLS} (whose additional, appended NLS at the C terminus further enhances nuclear localization) was even more effective than TrpRS in inducing p53-dependent phenotypes (**Supplementary Fig. 7b–d**) as well as in upregulation of the target mRNAs (**Supplementary Fig. 7e**). These results with single embryos were representative of similar analyses on additional embryos (wild-type, $n = 4$; TrpRS, $n = 10$; mini-TrpRS, $n = 6$; T2-TrpRS, $n = 6$; TrpRS^{NLS}, $n = 10$) and suggested that, in the presence of overexpressed TrpRS, the p53-driven apoptosis and senescence pathway is activated. This activation was apparent in the observed increases in acridine orange–positive or SA-β-gal–positive cells in embryonic phenotypes[40,41].

On the basis of the above findings, a mutually exclusive binding model for TrpRS and Ku70/80 with DNA-PK and PARP-1 in the nucleus is proposed in **Figure 6**. In the presence of Trp-AMP, the WHEP domain caps the active site, and Ku70/80 bridges between DNA-PK and PARP-1. However, in the presence of nuclear TrpRS and in the absence of Trp-AMP (as a result of IFN-γ stimulation), Ku70/80 is displaced as the 'flipped-out' WHEP domain bridges the C-terminal kinase domain of DNA-PKcs to the N-terminal domain of PARP-1. Consequently, PARylation of DNA-PKcs is stimulated, which in turn promotes the DNA-PKcs kinase activity for p53 phosphorylation and activation. Simultaneously, binding of TrpRS prevents Ku70/80 from binding DNA-PKcs and PARP-1 and subsequent phosphorylation of PARP-1 (**Fig. 6**).

DISCUSSION

In our work here, we detected a complex of DNA-PKcs–Ku70/80–PARP-1, which formed in the presence of damaged DNA, and of DNA-PKcs–TrpRS–PARP-1 (a DNA-independent ternary complex). Further work showed that the two complexes were mutually exclusive (**Fig. 2a,b**). Using different domains of PARP-1, we found that the CTD of PARP-1 interacts with the Ku70/80 bridging proteins and is phosphorylated by DNA-PKcs. In contrast, TrpRS bridged the N-terminal part of PARP-1 to the kinase domain of DNA-PKcs so that Ku70/80 and TrpRS differed in the way they oriented PARP-1 with respect to DNA-PKcs. In this orientation, DNA-PKcs was PARylated by PARP-1. Thus, the two orientations of DNA-PKcs and PARP-1 had different functional consequences.

The new orientation facilitated by TrpRS as a bridging protein occurs through the WHEP domains that are joined to the N termini of the homodimeric TrpRS subunits, with one binding partner (for example, DNA-PKcs) binding to one WHEP domain and the other partner (for example, PARP-1) to the other. TrpRS is one of ten class I tRNA synthetases, of which some (for example, CysRS, IleRS, LeuRS, ValRS, ArgRS GlnRS and GluRS) have monomeric structures, whereas others are dimers[2]. Although a complete active site is contained within each subunit of TrpRS, tRNA^{Trp} binds across the dimer interface so that the dimer is required for aminoacylation activity[21]. Remarkably, the function of TrpRS as a bridging protein for DNA-PKcs and PARP-1 provides a second rationale for the homodimeric structure of the synthetase. This homodimeric quaternary structure was conserved for TrpRSs throughout evolution[15]. Thus, the addition of the WHEP domain to TrpRS at the stage of vertebrate evolution exploited a preexisting dimeric state that could facilitate a bridging function for the synthetase.

The phosphorylation and activation of p53 described here seemed to be implemented, at least in part, by the nuclear TrpRS interaction with DNA-PKcs and PARP-1. This activation, through phosphorylation of Ser15, is linked to the robust antiangiogenic[32] and antiproliferative functions of p53 (ref. 42). Thus, the role of nuclear TrpRS may cooperate with its extracellular role as an angiostatic procytokine[12]. In addition, the possible activation of a major tumor suppressor by nuclear TrpRS is suggestive of a broader role that goes beyond angiostasis and is consistent with well-documented functional integration of IFN signaling and p53 activation[7,9,42].

Because overexpression of TrpRS was associated with p53 activation in the absence of IFN-γ stimulation (**Fig. 3d**) and because addition of the TrpRS-specific inhibitor Trp-SA, and not of another tRNA synthetase or protein-synthesis inhibitor, prevented IFN-γ–stimulated activation of p53 (**Fig. 4b**), TrpRS appears to have a role in IFN-γ–induced p53 activation. Its apparent role as a component of this functional integration may be part of the reason that TrpRS is strongly upregulated upon IFN-γ stimulation. Also of possible relevance is the long-standing and largely unexplained observation that IFN-γ stimulation upregulates tryptophan-degrading indoleamine 2,3-dioxygenase[43,44]. Our results suggest that nuclear TrpRS may link IFN-γ stimulation to p53 activation through emptying of the Trp-AMP–binding pocket to thereby promote a flipped-out position of the new WHEP domain that was added to TrpRSs at the stage of vertebrate evolution (**Fig. 4a–e**). Consequently, simultaneous upregulation of indoleamine 2,3-dioxygenase would promote activation of the nuclear role of TrpRS.

Notably, the work on LysRS[17] and the new results presented here on TrpRS show that at least some tRNA synthetases, long thought to have a role only in cytoplasmic translation, have distinct ex-translational nuclear functions. It remains a subject of future investigations to determine whether these functions originated from the need to coordinate these nuclear signaling pathways with translation in the cytoplasm.

METHODS

Cell culture, transfection and IFN-γ treatment. HeLa cells were cultured in a humidified incubator with 5% CO_2 in DMEM medium (Invitrogen) supplemented with 10% (v/v) FBS (Invitrogen) and 1× penicillin-streptomycin. The cells were transfected with pcDNA6-TrpRS-V5, pcDNA6-V5 or pcDNA3.1-ZZ-PARP-1 using Lipofectamine LTX (Invitrogen). To induce TrpRS expression by IFN-γ, the cells were incubated with human IFN-γ (R&D Systems) at a series of concentrations from 0–1,000 U ml^{-1} for 8–28 h before being used in experiments.

Recombinant protein purification. DNA encoding either full-length TrpRS (residues 1–471), mini-TrpRS (residues 48–471), T2-TrpRS (residues 94–471), N-terminal fragment (residues 1–186) or WHEP domain (residues 1–60) was cloned into NdeI and HindIII sites of pET-20b vector (Novagen). The expressed proteins include a His_6 tag from the vector sequence. The full-length PARP-1 and its variants (NTD and CTD) as well as the kinase domain of DNA-PKcs were cloned into pET 20b vector. All constructs were sequenced (Next Generation Sequencing Core Facility, The Scripps Research Institute, La Jolla) to confirm the success of cloning. All proteins having a C-terminal histidine tag were expressed in *E. coli* strain BL21 (DE3) by induction for 4 h with 1 mM isopropyl β-D-thiogalactopyranoside. Proteins were purified from the supernatants of lysed cells using Ni-NTA agarose (Qiagen) column chromatography according to manufacturer's instructions. ZZ-PARP-1, with an appended IgG-binding domain of Protein A at the N terminus, was purified from the HeLa cells after a 48-h transfection by binding IgG agarose beads. Immunoprecipitate was washed three times, subjected to SDS-PAGE and immunoblotted with PARP-1–specific antibody (BD Pharmingen, catalog no. 551024/7D3-6 and 1:1,000 dilution) to confirm the identity of the protein purified.

***In vitro* DNA-PK protein kinase activity assay.** DNA-PK protein kinase activity was measured per the manufacturer's assay protocol (Promega). In short, 5 µl recombinant TrpRS (0–25 µM) and 5 µl PARP-1 (1.25 mg ml^{-1}) were incubated with 5 µl DNA-PK (10 units) at 4 °C for 15 min, then incubated with 10 µl DNA-PK protein kinase assay cocktail (50 mM HEPES, pH 7.5, 100 mM KCl, 10 mM $MgCl_2$, 0.2 mM EGTA, 0.1 mM EDTA, 1 mM DTT, 2 µg ml^{-1} calf thymus DNA, 0.2 mM cold ATP, 40 µg ml^{-1} BSA and 1 µCi [γ-^{32}P]ATP (Perkin-Elmer)) at 30 °C for 30 min. DNA-PK–dependent phosphorylation of NTD-PARP-1 and CTD-PARP-1 (2 mg ml^{-1}) was conducted similarly as per the protocol in which they were used as substrate (10 µl each) for kinase activity. The reaction was stopped by addition of 25 µl 2× SDS sample buffer (5% v/v SDS, 10 mM DTT) and heated at 95 °C for 3 min. [^{32}P]PARP-1 or [^{32}P]CTD-PARP-1 was separated from free [γ-^{32}P]ATP on SDS-PAGE, dried and visualized by exposure to X-ray film. DNA-PK specific inhibitor KU57788 (catalog no. 1463), whenever used, was from Axon MedChem BV.

***In vitro* PARylation assay.** Twenty units of DNA-PK (Promega) was mixed with 5 µl recombinant TrpRS (0–5 µM) and 5 µl recombinant PARP-1 (2 µg) at 4 °C for 15 min and then incubated with 10 µl PAR assay cocktail (50 mM HEPES, pH 7.5, 100 mM KCl, 10 mM $MgCl_2$, 0.2 mM EGTA, 0.1 mM EDTA, 1 mM DTT, 200 nM NAD, 40 µg ml^{-1} BSA and 1 µCi [^{32}P]NAD (Perkin-Elmer)) at 30 °C for 30 min. The reaction was stopped by addition of 25 µl 2× SDS sample buffer (5% v/v SDS, 10 mM DTT) and heated at 95 °C for 3 min. The [^{32}P]PARylated DNA-PKcs was separated from free [^{32}P]NAD on SDS-PAGE, dried and visualized by exposure to X-ray film.

Acridine orange staining and detection of cell death in zebrafish embryos. Live zebrafish embryos were dechorionated in pronase (2.0 mg ml^{-1} in egg water, 5 mM NaCl, 0.17 mM KCl, 0.33 mM $CaCl_2$, 0.33 mM magnesium sulfate) for 3–5 min and rinsed five times in egg water at 28 h.p.f. At 30 h.p.f., embryos were incubated in 10 µg ml^{-1} acridine orange (Sigma A-6014) in egg water for 30 min at 28.5 °C, followed by three quick rinses. Embryos were anesthetized in 160 µg ml^{-1} tricaine (3-aminobenzoic acid ethyl ester, Sigma A-5040) and mounted laterally on the glass slide[41]. All zebrafish experiments were approved by and conducted in accordance with the guidelines established by the Institutional Animal Care and Use Committee at The Scripps Research Institute, with approval number 09-0009.

SA-β-gal activity assay in zebrafish embryos. Zebrafish embryos at 3.5 d post fertilization were washed in PBS and fixed overnight in 4% paraformaldehyde in PBS. After fixation, samples were washed twice in PBS (pH 7.5) and twice in PBS (pH 6.0) and then were incubated at 37 °C (in the absence of CO_2) for 12–16 h with SA-β-gal staining solution (5 mM potassium ferricyanide, 5 mM potassium ferrocyanide, 2 mM $MgCl_2$ in PBS at pH 6.0)[40].

Statistical analysis. Data processing and statistical analyses were performed using Statistical Package for the Social Sciences version 14.0. This software was used to perform statistical tests where appropriate.

Additional description of the experiments is provided in **Supplementary Methods**.

Received 2 September 2011; accepted 7 February 2012; published online 15 April 2012

References

1. Ling, J., Reynolds, N. & Ibba, M. Aminoacyl-tRNA synthesis and translational quality control. *Annu. Rev. Microbiol.* **63**, 61–78 (2009).
2. Carter, C.W. Jr. Cognition, mechanism, and evolutionary relationships in aminoacyl-tRNA synthetases. *Annu. Rev. Biochem.* **62**, 715–748 (1993).
3. Eriani, G., Delarue, M., Poch, O., Gangloff, J. & Moras, D. Partition of tRNA synthetases into two classes based on mutually exclusive sets of sequence motifs. *Nature* **347**, 203–206 (1990).
4. Fleckner, J., Rasmussen, H.H. & Justesen, J. Human interferon γ potently induces the synthesis of a 55-kDa protein (γ2) highly homologous to rabbit peptide chain release factor and bovine tryptophanyl-tRNA synthetase. *Proc. Natl. Acad. Sci. USA* **88**, 11520–11524 (1991).
5. Rubin, B.Y., Anderson, S.L., Xing, L., Powell, R.J. & Tate, W.P. Interferon induces tryptophanyl-tRNA synthetase expression in human fibroblasts. *J. Biol. Chem.* **266**, 24245–24248 (1991).
6. Bange, F.C., Flohr, T., Buwitt, U. & Bottger, E.C. An interferon-induced protein with release factor activity is a tryptophanyl-tRNA synthetase. *FEBS Lett.* **300**, 162–166 (1992).
7. Yang, G., Xu, Y., Chen, X. & Hu, G. IFITM1 plays an essential role in the antiproliferative action of interferon-γ. *Oncogene* **26**, 594–603 (2007).
8. Lindner, D.J. Interferons as antiangiogenic agents. *Curr. Oncol. Rep.* **4**, 510–514 (2002).
9. Kim, K.S., Kang, K.W., Seu, Y.B., Baek, S.H. & Kim, J.R. Interferon-γ induces cellular senescence through p53-dependent DNA damage signaling in human endothelial cells. *Mech. Ageing Dev.* **130**, 179–188 (2009).
10. Sgadari, C. *et al.* Mig, the monokine induced by interferon-γ, promotes tumor necrosis *in vivo*. *Blood* **89**, 2635–2643 (1997).
11. Angiolillo, A.L. *et al.* Human interferon-inducible protein 10 is a potent inhibitor of angiogenesis *in vivo*. *J. Exp. Med.* **182**, 155–162 (1995).
12. Wakasugi, K. *et al.* A human aminoacyl-tRNA synthetase as a regulator of angiogenesis. *Proc. Natl. Acad. Sci. USA* **99**, 173–177 (2002).
13. Kapoor, M. *et al.* Evidence for annexin II-S100A10 complex and plasmin in mobilization of cytokine activity of human TrpRS. *J. Biol. Chem.* **283**, 2070–2077 (2008).
14. Zhou, Q. *et al.* Orthogonal use of a human tRNA synthetase active site to achieve multifunctionality. *Nat. Struct. Mol. Biol.* **17**, 57–61 (2010).
15. Guo, M., Yang, X.L. & Schimmel, P. New functions of aminoacyl-tRNA synthetases beyond translation. *Nat. Rev. Mol. Cell Biol.* **11**, 668–674 (2010).
16. Sampath, P. *et al.* Noncanonical function of glutamyl-prolyl-tRNA synthetase: gene-specific silencing of translation. *Cell* **119**, 195–208 (2004).
17. Yannay-Cohen, N. *et al.* LysRS serves as a key signaling molecule in the immune response by regulating gene expression. *Mol. Cell* **34**, 603–611 (2009).
18. Popenko, V.I. *et al.* Immunoelectron microscopic location of tryptophanyl-tRNA synthetase in mammalian, prokaryotic and archaebacterial cells. *Eur. J. Cell Biol.* **62**, 248–258 (1993).

19. Popenko, V.I., Cherni, N.E., Beresten, S.F., Zargarova, T.A. & Favorova, O.O. Immune electron microscope determination of the localization of tryptophanyl-tRNA-synthetase in bacteria and higher eukaryotes. *Mol. Biol. (Mosk.)* **23**, 1669–1681 (1989).
20. Yang, X.L. *et al.* Functional and crystal structure analysis of active site adaptations of a potent anti-angiogenic human tRNA synthetase. *Structure* **15**, 793–805 (2007).
21. Yang, X.L. *et al.* Two conformations of a crystalline human tRNA synthetase-tRNA complex: implications for protein synthesis. *EMBO J.* **25**, 2919–2929 (2006).
22. Liu, J., Shue, E., Ewalt, K.L. & Schimmel, P. A new γ-interferon–inducible promoter and splice variants of an anti-angiogenic human tRNA synthetase. *Nucleic Acids Res.* **32**, 719–727 (2004).
23. Sibanda, B.L., Chirgadze, D.Y. & Blundell, T.L. Crystal structure of DNA-PKcs reveals a large open-ring cradle comprised of HEAT repeats. *Nature* **463**, 118–121 (2010).
24. Ariumi, Y. *et al.* Suppression of the poly(ADP-ribose) polymerase activity by DNA-dependent protein kinase *in vitro*. *Oncogene* **18**, 4616–4625 (1999).
25. Ruscetti, T. *et al.* Stimulation of the DNA-dependent protein kinase by poly(ADP-ribose) polymerase. *J. Biol. Chem.* **273**, 14461–14467 (1998).
26. Weterings, E. & Chen, D.J. DNA-dependent protein kinase in nonhomologous end joining: a lock with multiple keys? *J. Cell Biol.* **179**, 183–186 (2007).
27. Jin, S., Kharbanda, S., Mayer, B., Kufe, D. & Weaver, D.T. Binding of Ku and c-Abl at the kinase homology region of DNA-dependent protein kinase catalytic subunit. *J. Biol. Chem.* **272**, 24763–24766 (1997).
28. Lees-Miller, S.P., Sakaguchi, K., Ullrich, S.J., Appella, E. & Anderson, C.W. Human DNA-activated protein kinase phosphorylates serines 15 and 37 in the amino-terminal transactivation domain of human p53. *Mol. Cell. Biol.* **12**, 5041–5049 (1992).
29. Woo, R.A., McLure, K.G., Lees-Miller, S.P., Rancourt, D.E. & Lee, P.W. DNA-dependent protein kinase acts upstream of p53 in response to DNA damage. *Nature* **394**, 700–704 (1998).
30. Shieh, S.Y., Ikeda, M., Taya, Y. & Prives, C. DNA damage–induced phosphorylation of p53 alleviates inhibition by MDM2. *Cell* **91**, 325–334 (1997).
31. Beckert, S. *et al.* IGF-I-induced VEGF expression in HUVEC involves phosphorylation and inhibition of poly(ADP-ribose)polymerase. *Biochem. Biophys. Res. Commun.* **341**, 67–72 (2006).
32. Teodoro, J.G., Parker, A.E., Zhu, X. & Green, M.R. p53-mediated inhibition of angiogenesis through up-regulation of a collagen prolyl hydroxylase. *Science* **313**, 968–971 (2006).
33. Seburn, K.L., Nangle, L.A., Cox, G.A., Schimmel, P. & Burgess, R.W. An active dominant mutation of glycyl-tRNA synthetase causes neuropathy in a Charcot-Marie-Tooth 2D mouse model. *Neuron* **51**, 715–726 (2006).
34. Grueneberg, D.A. *et al.* Kinase requirements in human cells: IV. Differential kinase requirements in cervical and renal human tumor cell lines. *Proc. Natl. Acad. Sci. USA* **105**, 16490–16495 (2008).
35. Zhao, Y. *et al.* Preclinical evaluation of a potent novel DNA-dependent protein kinase inhibitor NU7441. *Cancer Res.* **66**, 5354–5362 (2006).
36. Aggad, D. *et al. In vivo* analysis of Ifn-γ1 and Ifn-γ2 signaling in zebrafish. *J. Immunol.* **185**, 6774–6782 (2010).
37. Sieger, D., Stein, C., Neifer, D., van der Sar, A.M. & Leptin, M. The role of γ interferon in innate immunity in the zebrafish embryo. *Dis. Model Mech.* **2**, 571–581 (2009).
38. Berghmans, S. *et al.* tp53 mutant zebrafish develop malignant peripheral nerve sheath tumors. *Proc. Natl. Acad. Sci. USA* **102**, 407–412 (2005).
39. Cao, L., Li, W., Kim, S., Brodie, S.G. & Deng, C.X. Senescence, aging and malignant transformation mediated by p53 in mice lacking the Brca1 full-length isoform. *Genes Dev.* **17**, 201–213 (2003).
40. Kishi, S. *et al.* The identification of zebrafish mutants showing alterations in senescence-associated biomarkers. *PLoS Genet.* **4**, e1000152 (2008).
41. Sidi, S. *et al.* Chk1 suppresses a caspase-2 apoptotic response to DNA damage that bypasses p53, Bcl-2 and caspase-3. *Cell* **133**, 864–877 (2008).
42. Takaoka, A. *et al.* Integration of interferon-α/β signalling to p53 responses in tumour suppression and antiviral defence. *Nature* **424**, 516–523 (2003).
43. Yoshida, R., Imanishi, J., Oku, T., Kishida, T. & Hayaishi, O. Induction of pulmonary indoleamine 2,3-dioxygenase by interferon. *Proc. Natl. Acad. Sci. USA* **78**, 129–132 (1981).
44. Yoshida, R., Urade, Y., Tokuda, M. & Hayaishi, O. Induction of indoleamine 2,3-dioxygenase in mouse lung during virus infection. *Proc. Natl. Acad. Sci. USA* **76**, 4084–4086 (1979).

Acknowledgments

We thank D. Chen (University of Texas Southwestern Medical School) for the DNA-PKcs clone and P. Chang (Massachusetts Institute of Technology) for the ZZ-PARP-1 clone. This work was supported by grants GM15539 and GM23562 (to P.S.) and GM088278 (to X.-L.Y.) from the US National Institutes of Health and by a fellowship from the National Foundation for Cancer Research.

Author contributions

M.S., Q.Z., S.K., D.M.V. Jr., M.K., M.G., S.L., S.K., X.-L.Y. and P.S. designed research; M.S., Q.Z., S.K., D.M.V. Jr., M.K. and S.L. carried out experiments; M.S., Q.Z., S.K., D.M.V. Jr., M.K., S.L., X.-L.Y. and P.S. analyzed data; and M.S., Q.Z., S.K., X.-L.Y. and P.S. wrote the paper.

Competing financial interests

The authors declare no competing financial interests.

Additional information

Supplementary information is available in the online version of the paper. Reprints and permissions information is available online at http://www.nature.com/reprints/index.html. Correspondence and requests for materials should be addressed to P.S.